Author Manuscript

Regional effects of gantenerumab on neuroimaging biomarkers in the DIAN-TU-001 trial

Austin McCullough [a*], Charles D. Chen [a*], Brian A. Gordon [a*], Nelly Joseph-Mathurin [a], Clifford R. Jack, Jr. [b], Robert Koeppe [c], Russ Hornbeck [a], Deborah Koudelis [a], Nicole S. McKay [a], Diana A. Hobbs [a], Shaney Flores [a], Sarah J. Keefe [a], Neelum T. Aggarwal [d], Ricardo F. Allegri [e], Sarah B. Berman [f], Thomas Bird [g], Sandra E. Black [h], William S. Brooks [i,j], Jasmeer P. Chhatwal [k], Gregory S. Day [l], Martin R. Farlow [m], Nick C. Fox [n], Serge Gauthier [o], Lawrence S. Honig [p], Ging-Yuek Hsiung [q], Mathias Jucker [r,s], Johannes Levin [t,u,v], Mario Masellis [h], Colin Masters [w], Patricio Chrem Mendez [e], John M. Ringman [x], B. Joy Snider [a], Stephen Salloway [y,z], Peter R. Schofield [i,j], Hiroyuki Shimada [aa], Kazushi Suzuki [bb], Christopher H. van Dyck [cc], Gregory Klein [dd], David B. Clifford [a], Carlos Cruchaga [a], Jason Hassenstab [a], Yan Li [a], Eric McDade [a], Susan Mills [a], John C. Morris [a], Richard J. Perrin [a], Charlene Supnet-Bell [a], Guoqiao Wang [a], Chengjie Xiong [a], Randall J. Bateman [a], Tammie L.S. Benzinger [a] for the DIAN-TU Study Team

[*]These authors contributed equally to the work.

Affiliations

[a] Washington University School of Medicine in Saint Louis, 660 S. Euclid Ave, St. Louis, MO 63110, USA

[b] Mayo Clinic, 200 First St. SW, Rochester, MN 55905, USA

[c] University of Michigan, 1301 Catherine St, Ann Arbor, MI 48109, USA

[d] Rush University Medical Center, 600 S. Paulina St., Chicago, IL 60612, USA

This is the author manuscript accepted for publication and has undergone full peer review but has not been through the copyediting, typesetting, pagination and proofreading process, which may lead to differences between this version and the Version of Record. Please cite this article as doi: /alz.70347

This article is protected by copyright. All rights reserved.

Author Manuscript

[e] Institute for Neurological Research FLENI, Montañeses 2325, Buenos Aires, Argentina

[f] University of Pittsburgh Medical Center, Pittsburgh, PA 15213, USA

[g] University of Washington, 1959 NE Pacific St, Seattle, WA 98195, USA

[h] Sunnybrook Health Sciences Centre, University of Toronto, 2075 Bayview Ave., Toronto, ON M4N 3M5, Canada

[i] Neuroscience Research Australia, 139 Barker St, Randwick NSW 2031, Australia

[j] The University of New South Wales, UNSW Sydney, NSW 2052, Australia

[k] Massachusetts General Hospital, Brigham and Women's Hospital, Harvard Medical School, 75 Francis St, Boston, MA 02115, USA

[l] Mayo Clinic, 4500 San Pablo Rd S, Jacksonville, FL 32224, USA

[m] Indiana University School of Medicine, 340 West 10th St, Indianapolis, IN 46202-3082, USA

[n] UK Dementia Research Institute and Dementia Research Centre, UCL Queen Square Institute of Neurology, University College London, London WC1E 6BT, UK

[o] McGill Center for Studies in Aging, McGill University, 6825, Boulevard LaSalle, Montréal, QC H4H 1R3, Canada

[p] Columbia University Irving Medical Center, 710 West 168th St, New York, NY 10032, USA

[q] University of British Columbia, 170-6371 Crescent Road, Vancouver, BC V6T 1Z2, Canada

[r] German Center for Neurodegenerative Diseases (DZNE), Otfried-Müller-Straße 23, 72076 Tübingen, Germany

[s] Hertie Institute for Clinical Brain Research, University of Tübingen, Otfried-Müller-Str. 27, 72076 Tübingen, Germany

[t] German Center for Neurodegenerative Diseases (DZNE), Feodor-Lynen-Strasse 17, 81377 Munich, Germany

This article is protected by copyright. All rights reserved.

Author Manuscript

[u] Ludwig Maximilian University of Munich, Geschwister-Scholl-Platz 1, 80539 Munich, Germany

[v] Munich Cluster for Systems Neurology (SyNergy), Feodor-Lynen-Str. 17, 81377 Munich, Germany

[w] University of Melbourne, Grattan St, Parkville VIC 3010, Australia

[x] Keck School of Medicine, University of Southern California, Los Angeles, CA 90033, USA

[y] Butler Hospital, 345 Blackstone Boulevard, Providence, RI 02906, USA

[z] Warren Alpert Medical School of Brown University, 222 Richmond St, Providence, RI 02903, USA

[aa] Osaka City University, 3-3-138, Sugimoto, Sumiyoshi-ku, Osaka-shi, 558-8585, Japan

[bb] National Defense Medical College, 3 Chome-2 Namiki, Tokorozawa, Saitama 359-8513, Japan

[cc] Yale School of Medicine, 333 Cedar St, New Haven, CT 06510, USA

[dd] Hoffmann-La Roche Ltd, Grenzacherstrasse 124, 4058 Basel, Switzerland

Corresponding Author:

Tammie L.S. Benzinger

Mallinckrodt Institute of Radiology

Washington University School of Medicine in St. Louis

Campus Box 8131

510 South Kingshighway Boulevard

This article is protected by copyright. All rights reserved.

St. Louis, MO 63110

Clinical Office Phone: (314) 362-5949

Research Office Phone: (314) 362-1558

benzingert@wustl.edu

Author Manuscript

This article is protected by copyright. All rights reserved.

Author Manuscript

Abstract

INTRODUCTION: Monoclonal anti-amyloid therapies are now accessible, but how these treatments influence changes within the brain is still not clear. We investigated overall and regional change in amyloid removal, glucose metabolism, and atrophy in trial participants with dominantly inherited Alzheimer disease (DIAD).

METHODS: In the DIAN-TU-001 trial, 92 carriers received gantenerumab or placebo and underwent serial neuroimaging assessments including [^{11}C]-Pittsburgh Compound-B (PiB) positron emission tomography (PET), [^{18}F]-Fluoro-2-deoxyglucose (FDG) PET, and magnetic resonance imaging (MRI).

RESULTS: Gantenerumab significantly reduced PiB-PET uptake overall and in most regions and showed no changes in FDG-PET or MRI measures. Drug effects were associated with baseline PiB-PET uptake and the largest effects occurred in medial regions.

DISCUSSION: Treated DIAD participants, and especially those with higher amyloid burden, showed decrease in PiB-PET uptake, which was more pronounced in the basal ganglia and medial frontal structures. These results may inform patient response and future drug trial design.

This article is protected by copyright. All rights reserved.

Author Manuscript

1. Introduction

Alzheimer disease (AD) is a progressive neurodegenerative disorder with a decades-long cascade of pathological changes preceding the onset of clinical symptoms. The formation of extracellular amyloid-beta (Aβ) plaques is hypothesized to initiate destructive cellular processes that culminate in widespread neuronal dysfunction and the buildup of neurofibrillary tangles (NFTs) primarily composed of hyperphosphorylated tau protein[1,2]. To date, clinical trials have focused primarily on Aβ-lowering therapies, given the prominence of Aβ early in the disease[3–5]. The primary approaches to lowering Aβ have been either the use of drugs that alter β-site amyloid precursor protein cleavage (BACE inhibitors[6–9]), or monoclonal antibody therapies that recognize monomeric (e.g. solanezumab[10,11]) or aggregated forms of Aβ (e.g. gantenerumab[12–14]). Despite initial promise, these trials mostly failed to meet their primary clinical endpoints unless amyloid was fully removed at an early stage of disease[15,16]. Possible reasons for failure include targeting the wrong protein aggregate, poor target engagement, inadequate or poorly optimized dosing, the influence of comorbidities in trial populations, and targeting individuals too late in the disease course[17–20].

Dominantly inherited Alzheimer disease (DIAD) is a rare form of AD caused by mutations in either the presenilin-1 (*PSEN1*), presenilin-2 (*PSEN2*), or amyloid precursor protein (*APP*) genes. In DIAD, age of symptomatic onset is heritable, highly predictable, and make DIAD a powerful model to study the pathogenesis and progression of AD[21]. Research with DIAD participants has shown that Aβ concentrations become abnormal decades before the onset of cognitive impairment, and that there are sequential downstream changes in tau phosphorylation, brain metabolism, structural declines in grey and white matter, and the formation of NFTs[22–27].

This article is protected by copyright. All rights reserved.

Author Manuscript

The Dominantly Inherited Alzheimer Network (DIAN) launched an observational study of DIAD in 2008[28,29] and the DIAN-Trials Unit (TU) was established in 2012 as a public-private collaboration[30–32]. The first trial (DIAN-TU-001) was launched in 2012 in asymptomatic and mildly symptomatic individuals to test the monoclonal Aβ antibody gantenerumab to abrogate disease progression in patients with DIAD[32]. The trial initially had a two-year biomarker endpoint that transitioned to a four-year treatment trial with a cognitive endpoint. Although the trial did not meet its cognitive endpoints within its four-year scope, the administration of gantenerumab lowered levels of cerebral Aβ measured using ^{11}C-Pittsburgh Compound B (^{11}C-PiB) positron emission tomography (PET)[33]. The observed longitudinal changes in volumetric estimates from MRI and brain metabolism assessed with FDG PET were not significantly different between placebo and drug arms when using the *a priori* defined summary measures, although significant reductions in CSF total tau and phospho-tau181 and slowed increases in CSF neurofilament light chain (NfL) concentrations were observed in the gantenerumab group relative to placebo[33].

Gantenerumab is a fully human monoclonal antibody that binds and removes aggregated Aβ by Fc receptor-mediated phagocytosis[34,35]. Early trials in patients with late-onset, sporadic AD found significant dose-dependent reductions in Aβ tracer uptake in participants receiving gantenerumab assessed using florbetapir PET[13,14]. A substudy of participants enrolled in the open-label extension of these trials with titration schedules up to 1200 mg every four weeks showed mean Aβ reduction levels of 90.3 Centiloids in the treatment naïve group and 57 and 74.9 Centiloids for the previously treated groups at year 3. These reductions resulted in 80% of participants having values below the amyloid positivity threshold[14]. The initial analyses of the DIAN-TU-001 data[33] looked only at prespecified summary neuroimaging variables and did not

This article is protected by copyright. All rights reserved.

account for regional heterogeneity. There is an urgent need to understand what impact anti-amyloid treatments have on amyloid-β plaques, glucose metabolism, and cortical atrophy in distinct regions of the brain to inform future drug trial and treatment plan design. Recognizing this, we aimed to assess how regional analysis of amyloid removal, glucose metabolism, and atrophy in the DIAN-TU-001 trial informed overall conclusions of 4-year gantenerumab treatment.

2. Materials and Methods

2.1.Participants

All data were collected during the DIAN-TU-001 trial (trial registration number: NCT01760005). Two-hundred-eleven participants were referred to DIAN-TU-001 from DIAN-OBS, DIAN Expanded Registry, DIAN-TU and partner sites. Eligibility criteria included participants known to have or to be at-risk for a DIAD mutation, to be between 15 years before to 10 years after the expected age of symptom onset (EYO), and to have received a Clinical Dementia Rating® (CDR) of 0 (cognitively normal) or 0.5 to 1 (early symptomatic cognitive impairment)[36]. Previously published demographics of this trial cohort[33] (see also Table 1) show that, although amyloid positivity was not explicitly part of the inclusion criteria, the vast majority of participants were amyloid positive at baseline due to the EYO range and mutation carrier status requirements. Participants could choose to remain blinded to their mutation status; mutation non-carriers were assigned to placebo groups. DIAD mutation carriers were randomized 3:1 to active or placebo with a minimization procedure[31,32,37]. All study participants, personnel, and sponsor were blinded to active or placebo assignment. Data from participants in the DIAN observational (DIAN-OBS) study who met the DIAN-TU inclusion criteria were used

This article is protected by copyright. All rights reserved.

Author Manuscript

to represent natural history controls for improved estimates of the placebo group. The DIAN-OBS and DIAN-TU have similar monitoring protocols, including cognitive, clinical, imaging and biomarker measures. Statistical evaluation of characteristics for all participants are provided in Table 1.

2.2.Study Design

DIAN-TU-001 was conducted at 25 sites in 7 countries, from December 2012 through November 2019. Investigators are listed in the supplementary information. Cognitive outcomes were assessed every 6 months, clinical outcomes annually, and biomarkers at baseline and at years 1, 2, and 4. A common close design ensured double-blind treatment continued for all participants until the last participant reached 4 years. Based on results of concurrent phase 2 and 3 trials in sporadic Alzheimer disease[13,14,38], target drug doses were increased approximately midway or later through the study. Gantenerumab was increased from 225 mg (subcutaneously, every 4 weeks) to 1200 mg in 2016[33].

Some participant dropout was observed over the course of the trial (Table 2). This can be attributed mainly to 1) participant dropout due to pathology advancement and 2) data loss due to rigorous imaging quality control measures. While the modeling strategy used attempts to account for this asymmetrical dropout, its potential effects on these results must be noted.

2.3.Imaging Methods

Magnetic resonance imaging (MRI) was performed using the Alzheimer's Disease Neuroimaging Initiative protocol. T1-weighted images (1.1 x 1.1 x 1.2 mm voxels) were acquired for all participants on a 3T MRI scanner. The DIAN MR and PET quality control (QC)

This article is protected by copyright. All rights reserved.

Author Manuscript

Author Manuscript

Cores screened images for protocol compliance, imaging artifacts, and amyloid related imaging abnormalities[39]. Volumetric segmentation and cortical surface reconstruction were completed using FreeSurfer v5.3 to define cortical and subcortical regions of interest[40,41]. Segmentations and surface reconstructions were visually inspected by members of the DIAN-TU Imaging Core and edited when needed. Subcortical volumes were corrected for intracranial volume using a regression approach[42]. Cortical thicknesses and subcortical volumes were summed across hemispheres.

Regions of interest (ROIs) defined by FreeSurfer on the MRI scans were used for the regional processing of all PET data. Aβ PET imaging was performed using ^{11}C-Pittsburgh Compound B (^{11}C-PiB), and ^{18}F-fluorodeoxyglucose (FDG) PET imaging was utilized as a marker of brain metabolism. Scans were processed using the PET Unified Pipeline (https://github.com/ysu001/PUP) that utilizes the regions of interest defined by FreeSurfer. PiB PET data from the 40-70 min post injection window and FDG data from the 40-60 min post injection window were converted to standardized uptake value ratios (SUVRs) using cerebellar grey matter as the reference region[43]. Data were partial volume corrected using a geometric transfer matrix approach[43,44]. A composite to represent a global measure of Aβ was calculated using the averaged SUVR values in the lateral orbitofrontal, medial orbitofrontal, precuneus, rostral middle frontal, superior frontal, superior temporal and middle temporal regions.

Voxel-wise mean SUVR images were generated by spatial normalizing participant images onto fsaverage in MNI space and calculating the arithmetic mean at each voxel for each group. The voxel-wise results were then surface-normal projected onto the atlas pial surface for visualization.

This article is protected by copyright. All rights reserved.

Author Manuscript

2.4.Statistical Analysis

Methods used to predetermine sample sizes and assign participants to arms were detailed in previous trial publications[31,33].

Linear mixed effects models (LME) were constructed in R v4.1.0 using lme4[45]. Model equations were structured as follows in pseudocode:

Imaging variable ~ baseline age + sex + apoe4 + baseline CDR + drug arm + baseline EYO + time in study + (*drug arm* × *baseline EYO*) + (*drug arm* × *time in study*) + (*time in study* | *subject*)

Random subject intercepts and slopes were included to accommodate individual variation. Models were performed with an unstructured covariance matrix to account for potential dependencies in longitudinal measurements. Models were constructed for the global summary measure of Aβ as well as for regional estimates of PiB, FDG, and structural MRI. FDR correction was used for multiple comparisons correction on regional analyses with statistical significance for all analyses set at a corrected $p < 0.05$. Regional analyses and brainmaps utilized the beta weight of the *drug arm* × *time in study* two-way interaction term from LME models to quantify the estimated longitudinal effect of gantenerumab use on imaging variables. An additional set of LME models were constructed identically except for a three-way interaction term (*drug arm* × *baseline EYO* × *time in study*) being included. This set of models was designed to test for potential changes in observed longitudinal drug effect as a function of disease state. Correlations of regional imaging variables with regional estimated drug effect beta weights were performed using a Pearson correlation.

This article is protected by copyright. All rights reserved.

Author Manuscript

3. Results

DIAD mutation carriers were randomized 3:1 to gantenerumab or placebo drug arms with a robust minimization procedure[37] as previously described[31,33]. This procedure minimized between-group differences at baseline in all relevant participant statistics including genetic, cognitive, imaging, and disease state categories (Table 1). At baseline, 58% of participants were considered cognitively unimpaired (CDR 0) and 42% of participants were considered cognitively impaired (CDR >0). Baseline mean amyloid burden across the groups was 64 Centiloids with a wide standard deviation reflecting a large within-group diversity of disease states while maintaining between-group integrity (Table 1).

Analysis on the subset of participants who completed the entire 4-year trial course resulted in a reduction of average mean cortical PiB PET signal from 2.49 SUVR (64.6 Centiloids) at baseline to 2.09 SUVR (46.6 Centiloids) at year 4 in the gantenerumab group, as opposed to a rise from 2.27 SUVR (54.2 Centiloids) at baseline to 2.61 SUVR (70.0 Centiloids) at year 4 in the placebo group. Figure 1 illustrates the voxel-wise cortical PiB PET SUVR values in gantenerumab and placebo groups in trial completers using non-partial-volume corrected data.

LME model analysis on the entire trial dataset revealed that treatment with gantenerumab significantly reduced the longitudinal increase of mean cortical PiB PET signal (β = -.15, *SE* = .026, *df* =71.26, *t* = -5.88, *p(fdr)* = 4.68_{10}^{-07} *[benefit is neg.]*) relative to the placebo group (Table 2). Additionally, gantenerumab treatment significantly reduced longitudinal PiB PET in 32 of 34 cortical and 7 of 9 subcortical regions examined (Table 3). The effect strength of gantenerumab on longitudinal PiB PET values varied considerably, with the most significant effects seen in the dorsal striatum (caudate β = -.35, *SE* = .045, *df* = 77.03, *t* = -7.91, *p(fdr)* = 3.39_{10}^{-10} ; putamen β =

This article is protected by copyright. All rights reserved.

-.28, *SE* = .035, *df* = 77.02, *t* = -8.04, *p(fdr)* = 3.39_{10}^{-10}), thalamus (*β* = -.17, *SE* = .024, *df* = 82.17, *t* = -6.92, *p(fdr)* = 1.31_{10}^{-08}), anterior cingulate (rostral anterior cingulate *β* = -.23, *SE* = .034, *df* = 69.47, *t* = -6.89, *p(fdr)* = 1.90_{10}^{-08} ; caudal anterior cingulate *β* = -.23, *SE* = .034, *df* = 69.20, *t* = -6.88, *p(fdr)* = 1.90_{10}^{-08}) and medial orbitofrontal (*β* = -.21, *SE* = .033, *df* = 77.46, *t* = -6.34, *p(fdr)* = 1.02_{10}-^{07}) regions (Table 3, Figure 2A, Figure 3).

Many of the regions with high drug effects also displayed prominent baseline PiB PET signal, although posterior cortical structures with prominent baseline PiB PET signal showed noticeably smaller, but still significant drug effects (precuneus *β* = -.16, *SE* = .031, *df* = 70.19, *t* = -5.27, *p(fdr)* = 4.00_{10}^{-06}; posterior cingulate *β* = -.17, *SE* = .032, *df* = 63.47, *t* = -5.26, *p(fdr)* = 4.60_{10}^{-06}; isthmus cingulate *β* = -.11, *SE* = .023, *df* = 65.77, *t* = -4.75, *p(fdr)* = 2.08_{10}^{-05}) (Figure 2B, Figure 3). Figure 3 corroborates the regional model results by showing baseline normalized end of trial PiB PET SUVR values for four key regions displaying a large variance in beta weight values of the drug x time model component (Figure 3). A direct correlation between regional estimated drug effect values to regional baseline estimates of pathology revealed a Pearson correlation of *r(43)* = 0.75, *p* = 2_{10}^{-08} with several subcortical structures having outsized model beta weights relative to their baseline PiB PET levels (Figure 2C). No statistically significant differences between gantenerumab and placebo arms were found in the regional analyses for PiB when applying the three-way interaction (Table S1). Although biomarker changes in FDG and MRI metrics were observed over the course of the trial consistent with established yearly changes in these biomarkers at early preclinical stage of the disease[33], no significant differences were found in any regional analysis between gantenerumab and placebo arms in FDG and MRI (Table S2, Table S3a, Table S3b).

This article is protected by copyright. All rights reserved.

Author Manuscript

Author Manuscript

4. Discussion

Top-line results from the DIAN-TU-001 trial demonstrated a significant effect of gantenerumab on global Aβ load clearance[33]. The current analyses establish that the estimated efficacy of gantenerumab was not homogenous across the brain but varied by region, with the greatest effects observed in the dorsal striatum, thalamus, nucleus accumbens, caudal anterior cingulate, rostral anterior cingulate, and medial frontal regions (Table 3, Figure 2A, Figure 3). Recognizing and understanding what drives these spatial patterns is of high interest to inform future clinical trials, as it may elucidate the way the drug is behaving in the brain.

A major contributing factor to these regional differences is the baseline level of Aβ pathology in each region prior to drug administration as evident by the spatial similarity between the two (Figure 2A&B). However, data presented here suggests this relationship does not fully explain the regional differences in estimated drug effects (Figure 2C, Figure 3). In both sporadic AD and DIAD, posterior parietal regions are one of the earliest regions to demonstrate Aβ deposition and reach the highest levels of pathology accumulation[24,46]. In DIAD many participants also show substantial buildup of Aβ in the dorsal striatum, although to a lesser extent than both parietal and medial frontal regions[24,46,47]. The current results show the greatest estimated drug effect was seen in the dorsal striatum, thalamus, nucleus accumbens, anterior cingulate, and medial frontal regions of the brain with more modest, albeit significant, effects in posterior parietal regions (Table 3, Figure 2A). In particular, several subcortical structures showed relatively high regional model beta weights relative to their baseline amyloid pathology levels (Figure 2), and display larger average reductions in PiB PET SUVR values at end of trial relative to other regions (Figure 2,3). This suggests that drug effects are not solely proportional to baseline levels of amyloid pathology and are being influenced by other factors.

This article is protected by copyright. All rights reserved.

Author Manuscript

Given that regional differences in uptake between Aβ tracers have been documented in this cohort, and that regional cortical rates of change in ^{11}C-PiB decreased more rapidly than ^{18}F-Florbetapir in both placebo and gantenerumab group[48], it is possible that some of this relationship is due to the use of ^{11}C-PiB as the tracer of choice. However, drug effects remained highly significant across both Aβ tracers and recapitulated a very similar spatial pattern regardless of the tracer used[48].

The observed spatial pattern may be driven by a unique feature of the DIAD cohort. Prior work has shown that Aβ accrual in the dorsal striatum is a feature of DIAD as well as Down syndrome (associated with triplication of *APP*)[47], and is present, but at much lower levels, in sporadic AD[49,50]. This could explain why these regions have some of the greatest reductions in the current analyses. However, evidence from previous trials in sporadic AD using gantenerumab also show similar regional variability, with prominent regional reductions in Aβ in the dorsal striatum, anterior cingulate, and medial frontal regions[14,38]. The consistent spatial patterns suggest a common mechanism.

If the pattern is not driven by the cohort, then it is likely tied to properties of the specific regions. Previous research has demonstrated that blood flow levels vary regionally across the brain[51], and this could cause different levels of drug delivery, and therefore pathology clearance. Additionally, it may not be overall blood flow that determines drug access, but rather blood-brain-barrier (BBB) permeability[52]. Anecdotal evidence from clinical trials has shown incidences where amyloid related imaging abnormalities were associated with a corresponding local clearance of plaques interpreted as being due to increased drug accessibility[34,53]. Finally, there is evidence that lymphatic systems play a role in regulating CSF flow in the brain[54]. It may be that

This article is protected by copyright. All rights reserved.

Author Manuscript

regional exposure to the drug is modulated by both blood flow as well as subsequent clearance from the brain.

Histopathological examinations have classified an array of different plaque types occurring in the brain, potentially representing different stages in the life cycle of plaque development[55–57] and this evolution varies regionally in the brain[58]. Pharmacodynamic studies of gantenerumab show specific binding to fibrillar Aβ at sites on the N-terminal and spatially adjacent central Aβ sequences[12,35]. Thus, gantenerumab may display a different affinity for, and therefore a different clearance rate, for each specific type of Aβ plaque depending upon the availability of these binding sites. Such a phenomenon may explain why medial frontal regions and basal ganglia structures displayed higher drug effects and parietal structures displayed lower estimated drug effect levels, respectively, than their baseline levels of Aβ load would suggest.

Although we found significant reduction in PiB PET signal during the four-year trial period, we found no evidence of significant drug effects on the downstream imaging markers of FDG PET or MRI. Prior analyses of cerebrospinal fluid during the trial did reveal decreases in CSF total tau and phospho-tau181 levels, and blunted increases in CSF NfL levels[33], indicating at least some modification of neurodegeneration processes. This lack of effect on these imaging measures could be due to multiple causes. First, imaging measures specifically are known to be aggregate measures that include prior damage, therefore downstream effects take a longer time to become apparent[23–27]. The four-year trial length, coupled with the dose escalation protocol mid-trial, meant that participants only received the highest doses of gantenerumab between years 2 and 4[33]. Marked increases in Aβ clearance were observed during this time, suggesting that even more significant effects of gantenerumab could have been observed if higher doses were administered throughout the trial. Second, despite significant reductions, a large majority of

This article is protected by copyright. All rights reserved.

Author Manuscript

participants still had abnormal levels of Aβ as measured by both PiB PET signal and CSF. It may be only when levels of Aβ deposits are sufficiently reduced to normal levels or when enough bulk amyloid has been removed from the brain that neurodegenerative markers substantially improve. Additionally, the relatively low N of the trial coupled with progressively losing some high pathology participants due to asymmetrical dropout could negatively affect the ability of this analysis to identify any biomarker changes beyond the strongest effects. Finally, tau PET imaging was introduced late in the trial, preventing us from relating amyloid reductions to this key marker of neurofibrillary pathology. The extension of the DIAN TU-001 into a three-year open-label extension will address these key questions.

In conclusion, treatment with gantenerumab significantly reduced global PiB PET signal in DIAD participants over a four-year trial period. This estimated drug effect was not ubiquitous across the brain but varied regionally, with the highest levels of signal reduction in the dorsal striatum, thalamus, nucleus accumbens, caudal anterior cingulate, rostral anterior cingulate, and medial frontal regions. Regional variations in PiB signal change were positively correlated with, but not solely explained by, levels of baseline Aβ pathology present in each region. We did not find any evidence of improvement in downstream metabolic or neurodegeneration imaging biomarkers over the four-year trial period. These findings suggest that prolonged use of gantenerumab is effective in significantly reducing PiB PET signal, although future work is needed to evaluate whether reductions in Aβ can effect changes in clinical and neurodegenerative trajectories.

References

This article is protected by copyright. All rights reserved.

Author Manuscript

1. Jack CR, Bennett DA, Blennow K, et al. NIA-AA Research Framework: Toward a biological definition of Alzheimer's disease. *Alzheimers Dement*. 2018;14(4):535-562. doi:10.1016/j.jalz.2018.02.018

2. Braak H, Thal DR, Ghebremedhin E, Del Tredici K. Stages of the Pathologic Process in Alzheimer Disease: Age Categories From 1 to 100 Years. *J Neuropathol Exp Neurol*. 2011;70(11):960-969. doi:10.1097/NEN.0b013e318232a379

3. Hardy J, Selkoe DJ. The amyloid hypothesis of Alzheimer's disease: progress and problems on the road to therapeutics. *Science*. 2002;297(5580):353-356. doi:10.1126/science.1072994

4. Karran E, Mercken M, Strooper BD. The amyloid cascade hypothesis for Alzheimer's disease: an appraisal for the development of therapeutics. *Nat Rev Drug Discov*. 2011;10(9):698-712. doi:10.1038/nrd3505

5. Barage SH, Sonawane KD. Amyloid cascade hypothesis: Pathogenesis and therapeutic strategies in Alzheimer's disease. *Neuropeptides*. 2015;52:1-18. doi:10.1016/j.npep.2015.06.008

6. Egan MF, Kost J, Tariot PN, et al. Randomized Trial of Verubecestat for Mild-to-Moderate Alzheimer's Disease. *N Engl J Med*. 2018;378(18):1691-1703. doi:10.1056/NEJMoa1706441

7. Neumann U, Ufer M, Jacobson LH, et al. The BACE -1 inhibitor CNP 520 for prevention trials in Alzheimer's disease. *EMBO Mol Med*. 2018;10(11):e9316. doi:10.15252/emmm.201809316

8. Henley D, Raghavan N, Sperling R, Aisen P, Raman R, Romano G. Preliminary Results of a Trial of Atabecestat in Preclinical Alzheimer's Disease. *N Engl J Med*. 2019;380(15):1483-1485. doi:10.1056/NEJMc1813435

9. Lo AC, Evans CD, Mancini M, et al. Phase II (NAVIGATE-AD study) Results of LY3202626 Effects on Patients with Mild Alzheimer's Disease Dementia. *Journal of Alzheimer's Disease Reports*. 2021;5(1):321-336. doi:10.3233/ADR-210296

10. Dodart JC, Bales KR, Gannon KS, et al. Immunization reverses memory deficits without reducing brain Aβ burden in Alzheimer's disease model. *Nat Neurosci*. 2002;5(5):452-457. doi:10.1038/nn842

11. Honig LS, Vellas B, Woodward M, et al. Trial of Solanezumab for Mild Dementia Due to Alzheimer's Disease. *N Engl J Med*. 2018;378(4):321-330. doi:10.1056/NEJMoa1705971

12. Bohrmann B, Baumann K, Benz J, et al. Gantenerumab: A Novel Human Anti-Aβ Antibody Demonstrates Sustained Cerebral Amyloid-β Binding and Elicits Cell-Mediated Removal of Human Amyloid-β. *JAD*. 2012;28(1):49-69. doi:10.3233/JAD-2011-110977

13. Ostrowitzki S, Lasser RA, Dorflinger E, et al. A phase III randomized trial of gantenerumab in prodromal Alzheimer's disease. *Alz Res Therapy*. 2017;9(1):95. doi:10.1186/s13195-017-0318-y

This article is protected by copyright. All rights reserved.

Author Manuscript

14. Klein G, Delmar P, Voyle N, et al. Gantenerumab reduces amyloid-β plaques in patients with prodromal to moderate Alzheimer's disease: a PET substudy interim analysis. *Alz Res Therapy*. 2019;11(1):101. doi:10.1186/s13195-019-0559-z

15. Mintun MA, Lo AC, Duggan Evans C, et al. Donanemab in Early Alzheimer's Disease. *N Engl J Med*. 2021;384(18):1691-1704. doi:10.1056/NEJMoa2100708

16. Van Dyck CH, Swanson CJ, Aisen P, et al. Lecanemab in Early Alzheimer's Disease. *N Engl J Med*. 2023;388(1):9-21. doi:10.1056/NEJMoa2212948

17. Mehta D, Jackson R, Paul G, Shi J, Sabbagh M. Why do trials for Alzheimer's disease drugs keep failing? A discontinued drug perspective for 2010-2015. *Expert Opinion on Investigational Drugs*. 2017;26(6):735-739. doi:10.1080/13543784.2017.1323868

18. Anderson RM, Hadjichrysanthou C, Evans S, Wong MM. Why do so many clinical trials of therapies for Alzheimer's disease fail? *The Lancet*. 2017;390(10110):2327-2329. doi:10.1016/S0140-6736(17)32399-1

19. Parasrampuria DA, Benet LZ, Sharma A. Why Drugs Fail in Late Stages of Development: Case Study Analyses from the Last Decade and Recommendations. *AAPS J*. 2018;20(3):46. doi:10.1208/s12248-018-0204-y

20. Yiannopoulou KG, Anastasiou AI, Zachariou V, Pelidou SH. Reasons for Failed Trials of Disease-Modifying Treatments for Alzheimer Disease and Their Contribution in Recent Research. *Biomedicines*. 2019;7(4):97. doi:10.3390/biomedicines7040097

21. Rabinovici GD. Dominantly inherited Alzheimer's disease: a compass for drug development. *Nat Med*. 2021;27(7):1148-1150. doi:10.1038/s41591-021-01434-2

22. Bateman RJ, Xiong C, Benzinger TLS, et al. Clinical and Biomarker Changes in Dominantly Inherited Alzheimer's Disease. *N Engl J Med*. 2012;367(9):795-804. doi:10.1056/NEJMoa1202753

23. Ryman DC, Acosta-Baena N, Aisen PS, et al. Symptom onset in autosomal dominant Alzheimer disease: A systematic review and meta-analysis. *Neurology*. 2014;83(3):253-260. doi:10.1212/WNL.0000000000000596

24. Gordon BA, Blazey TM, Su Y, et al. Spatial patterns of neuroimaging biomarker change in individuals from families with autosomal dominant Alzheimer's disease: a longitudinal study. *The Lancet Neurology*. 2018;17(3):241-250. doi:10.1016/S1474-4422(18)30028-0

25. Li D, Donohue MC. Disease progression models for dominantly-inherited Alzheimer's disease. *Brain*. 2018;141(5):1244-1246. doi:10.1093/brain/awy089

26. McDade E, Wang G, Gordon BA, et al. Longitudinal cognitive and biomarker changes in dominantly inherited Alzheimer disease. *Neurology*. 2018;91(14). doi:10.1212/WNL.0000000000006277

This article is protected by copyright. All rights reserved.

Author Manuscript

27. Oxtoby NP, Young AL, Cash DM, et al. Data-driven models of dominantly-inherited Alzheimer's disease progression. *Brain*. 2018;141(5):1529-1544. doi:10.1093/brain/awy050

28. Bateman RJ, Aisen PS, De Strooper B, et al. Autosomal-dominant Alzheimer's disease: a review and proposal for the prevention of Alzheimer's disease. *Alzheimers Res Ther*. 2011;3(1):1. doi:10.1186/alzrt59

29. Morris JC, Aisen PS, Bateman RJ, et al. Developing an international network for Alzheimer research: The Dominantly Inherited Alzheimer Network. *Clin Investig (Lond)*. 2012;2(10):975-984. doi:10.4155/cli.12.93

30. Moulder KL, Snider BJ, Mills SL, et al. Dominantly Inherited Alzheimer Network: facilitating research and clinical trials. *Alzheimers Res Ther*. 2013;5(5):48. doi:10.1186/alzrt213

31. Mills SM, Mallmann J, Santacruz AM, et al. Preclinical trials in autosomal dominant AD: Implementation of the DIAN-TU trial. *Revue Neurologique*. 2013;169(10):737-743. doi:10.1016/j.neurol.2013.07.017

32. Bateman RJ, Benzinger TL, Berry S, et al. The DIAN-TU Next Generation Alzheimer's prevention trial: Adaptive design and disease progression model. *Alzheimer's & Dementia*. 2017;13(1):8-19. doi:10.1016/j.jalz.2016.07.005

33. Salloway S, Farlow M, McDade E, et al. A trial of gantenerumab or solanezumab in dominantly inherited Alzheimer's disease. *Nat Med*. 2021;27(7):1187-1196. doi:10.1038/s41591-021-01369-8

34. Ostrowitzki S. Mechanism of Amyloid Removal in Patients With Alzheimer Disease Treated With Gantenerumab. *Arch Neurol*. 2012;69(2):198. doi:10.1001/archneurol.2011.1538

35. Novakovic D, Feligioni M, Scaccianoce S, et al. Profile of gantenerumab and its potential in the treatment of Alzheimer's disease. *Drug Des Devel Ther*. 2013;7:1359-1364. doi:10.2147/DDDT.S53401

36. Morris JC. The Clinical Dementia Rating (CDR): current version and scoring rules. *Neurology*. 1993;43(11):2412-2414. doi:10.1212/wnl.43.11.2412-a

37. Taves DR. Minimization: A new method of assigning patients to treatment and control groups. *Clin Pharma and Therapeutics*. 1974;15(5):443-453. doi:10.1002/cpt1974155443

38. Klein G, Delmar P, Kerchner GA, et al. Thirty-Six-Month Amyloid Positron Emission Tomography Results Show Continued Reduction in Amyloid Burden with Subcutaneous Gantenerumab. *The Journal of Prevention of Alzheimer's Disease*. 2021;8(1):3-6. doi:10.14283/jpad.2020.68

This article is protected by copyright. All rights reserved.

Author Manuscript

39. Sperling R, Salloway S, Brooks DJ, et al. Amyloid-related imaging abnormalities in patients with Alzheimer's disease treated with bapineuzumab: a retrospective analysis. *The Lancet Neurology*. 2012;11(3):241-249. doi:10.1016/S1474-4422(12)70015-7

40. Fischl B. Automatically Parcellating the Human Cerebral Cortex. *Cerebral Cortex*. 2004;14(1):11-22. doi:10.1093/cercor/bhg087

41. Fischl B. FreeSurfer. *NeuroImage*. 2012;62(2):774-781. doi:10.1016/j.neuroimage.2012.01.021

42. Buckner RL, Head D, Parker J, et al. A unified approach for morphometric and functional data analysis in young, old, and demented adults using automated atlas-based head size normalization: reliability and validation against manual measurement of total intracranial volume. *NeuroImage*. 2004;23(2):724-738. doi:10.1016/j.neuroimage.2004.06.018

43. Su Y, Blazey TM, Snyder AZ, et al. Partial volume correction in quantitative amyloid imaging. *NeuroImage*. 2015;107:55-64. doi:10.1016/j.neuroimage.2014.11.058

44. Funck T, Paquette C, Evans A, Thiel A. Surface-based partial-volume correction for high-resolution PET. *NeuroImage*. 2014;102:674-687. doi:10.1016/j.neuroimage.2014.08.037

45. Bates D, Mächler M, Bolker B, Walker S. Fitting Linear Mixed-Effects Models Using **lme4**. *J Stat Soft*. 2015;67(1). doi:10.18637/jss.v067.i01

46. Benzinger TLS, Blazey T, Jack CR, et al. Regional variability of imaging biomarkers in autosomal dominant Alzheimer's disease. *Proc Natl Acad Sci USA*. 2013;110(47). doi:10.1073/pnas.1317918110

47. Cohen AD, McDade E, Christian B, et al. Early striatal amyloid deposition distinguishes Down syndrome and autosomal dominant Alzheimer's disease from late-onset amyloid deposition. *Alzheimer's & Dementia*. 2018;14(6):743-750. doi:10.1016/j.jalz.2018.01.002

48. Chen CD, McCullough A, Gordon B, et al. Longitudinal head-to-head comparison of 11C-PiB and 18F-florbetapir PET in a Phase 2/3 clinical trial of anti-amyloid-β monoclonal antibodies in dominantly inherited Alzheimer's disease. *Eur J Nucl Med Mol Imaging*. 2023;50(9):2669-2682. doi:10.1007/s00259-023-06209-0

49. Hanseeuw BJ, Betensky RA, Mormino EC, et al. PET staging of amyloidosis using striatum. *Alzheimer's & Dementia*. 2018;14(10):1281-1292. doi:10.1016/j.jalz.2018.04.011

50. Chen CD, Joseph-Mathurin N, Sinha N, et al. Comparing amyloid-β plaque burden with antemortem PiB PET in autosomal dominant and late-onset Alzheimer disease. *Acta Neuropathol*. 2021;142(4):689-706. doi:10.1007/s00401-021-02342-y

51. Herscovitch P, Markham J, Raichle ME. Brain blood flow measured with intravenous H2(15)O. I. Theory and error analysis. *J Nucl Med*. 1983;24(9):782-789.

This article is protected by copyright. All rights reserved.

Author Manuscript

52. Banks WA. Drug delivery to the brain in Alzheimer's disease: Consideration of the blood–brain barrier. *Advanced Drug Delivery Reviews*. 2012;64(7):629-639. doi:10.1016/j.addr.2011.12.005

53. Joseph-Mathurin N, Llibre-Guerra JJ, Li Y, et al. Amyloid-Related Imaging Abnormalities in the DIAN-TU-001 Trial of Gantenerumab and Solanezumab: Lessons from a Trial in Dominantly Inherited Alzheimer Disease. *Ann Neurol*. 2022;92(5):729-744. doi:10.1002/ana.26511

54. Iliff JJ, Wang M, Liao Y, et al. A Paravascular Pathway Facilitates CSF Flow Through the Brain Parenchyma and the Clearance of Interstitial Solutes, Including Amyloid β. *Sci Transl Med*. 2012;4(147). doi:10.1126/scitranslmed.3003748

55. Armstrong RA. β-Amyloid Plaques: Stages in Life History or Independent Origin? *Dement Geriatr Cogn Disord*. 1998;9(4):227-238. doi:10.1159/000017051

56. D'Andrea M, Nagele R. Morphologically distinct types of amyloid plaques point the way to a better understanding of Alzheimer's disease pathogenesis. *Biotechnic & Histochemistry*. 2010;85(2):133-147. doi:10.3109/10520290903389445

57. Röhr D, Boon BDC, Schuler M, et al. Label-free vibrational imaging of different Aβ plaque types in Alzheimer's disease reveals sequential events in plaque development. *Acta Neuropathol Commun*. 2020;8(1):222. doi:10.1186/s40478-020-01091-5

58. Thal DR, Capetillo-Zarate E, Del Tredici K, Braak H. The Development of Amyloid β Protein Deposits in the Aged Brain. *Sci Aging Knowl Environ*. 2006;2006(6). doi:10.1126/sageke.2006.6.re1

Consent Statement

All participants or their caregivers provided written informed consent approved by their local institution's review board.

Keywords: Autosomal dominant Alzheimer disease (ADAD); Dominantly inherited Alzheimer's disease (DIAD); DIAN-TU; Amyloid targeted monoclonal antibody; Gantenerumab; regional variability; PET; Regional PiB-PET uptake; FDG-PET; MRI measures; imaging outcomes.

This article is protected by copyright. All rights reserved.

Author Manuscript

Acknowledgements, Sources of Funding, and Disclosures

a) Acknowledgements: This manuscript has been reviewed by DIAN-TU study investigators for scientific content and consistency of data interpretation with previous DIAN-TU study publications. We acknowledge the altruism of the participants and their families and contributions of the DIAN research and support staff at each of the participating sites for their contributions to this study.

b) Sources of Funding: Research reported in this publication was supported by the National Institute on Aging of the National Institutes of Health under Award Numbers U01AG042791, U01AG042791-S1 (FNIH and Accelerating Medicines Partnership), R01AG046179, R01AG053267, R01AG053267-S1, R01AG053267-S2. The research for the DIAN-TU-001 gantenerumab open label extension was supported by the Alzheimer's Association and F. Hoffman-LaRoche Ltd. The research for the DIAN-TU-001 trial, solanezumab and gantenerumab drug arms, was also supported by the Alzheimer's Association, Eli Lilly and Company, F. Hoffman-LaRoche Ltd., Avid Radiopharmaceuticals (a wholly owned subsidiary of Eli Lilly and Company), GHR Foundation, an anonymous organization, Cerveau Technologies, Cogstate, and Signant. AM acknowledges support from the NIH (T32AG078117-01). NJM acknowledges support from the NIH (1K01AG080123), and Alzheimer's Association (AARFD-20-681815).

c) Disclosures: NJM received travel support from the Alzheimer's Association to present at AAIC and an honorarium from the PeerView Institute for Medical Education for participating as a facilitator in training workshops at AAIC. CRJ served on a DSMB for Roche with no compensation. NSM acknowledges support from BrightFocus (A2022013F) and Alzheimer's

This article is protected by copyright. All rights reserved.

Association (AARF-21-722077), received honoraria from PeerView Institute for Medical Education for participating as a facilitator in training workshops at AAIC. NTA acknowledges institutional support from Eisai, Lilly, Pfizer, and Roche. RFA acknowledges institutional aupport from Alzheimer's Association (LatamFINGER, iLEADS), and Washington University in St. Louis. SEB acknowledges institutional support from Genentech, Optina, Roche, Lilly, Eisai/Biogen Idec, NovoNordisk, Lilly Avid, ICON, Aribio Co, Ontario Brain Institute, CIHR, Leducq Foundation, Heart and Stroke Foundation of Canada, Brain Canada, Weston Brain Institute, Canadian Partnership for Stroke Recovery, Canadian Foundation for Innovation, Focused Ultrasound Foundation, Alzheimer's Association US, Queen's University, Compute Canada Resources for Research Groups, CANARIE, Networks of Centres of Excellence Canada, and received consulting fees from Roche, Biogen, NovoNordisk, Eisai, Eli Lilly, and DSR, as well as support for presentations from Biogen, Roche, and Eisai. WSB received support for a presentation at Dementia Trials Australia Annual scientific meeting. JC received consulting fees from Humana, MedaCorp, and ExpertConnect. GSD acknowledges institutional support from NIH (R01AG089380, K23AG064029, U01NS120901, U01AG057195, U19AG032438), and received consulting fees from Parabon Nanolabs and Arialys Pharmaceuticals, support for presentations from PeerView Media, Continuing Education Inc., Eli Lilly, Ionis Pharmaceuticals, and DynaMed, personal compensation from ANI Pharmaceuticals, and material support of clinical trial (NCT04372615) from Amgen Therapeutics. MF received support for conduct of clinical trials from Eli Lilly, Roche/Genentech, Avanir, Biogen, Cognition Therapeutics, Green Valley, Otsuka, Neurotrope Biosciences, AZTherapies, Athira, Ionis, and Lexeo. NCF received consulting fees from Eisai, Roche, Eli Lilly, and Biogen, and support for presentations from Roche. SG received consulting fees from AmyriAD, Eisai Canada, Enigma USA, Lilly Canada,

This article is protected by copyright. All rights reserved.

Author Manuscript

Author Manuscript

Nordisk Canada, TauRx, and support for presentations from Otsuka Canada, and Lilly Canada. LSH acknowledges institutional support from Abbvie, Acumen, Alector, AstraZeneca, Avanir, Axovant, Biogen, Bristol-Myer Squibb, Eisai, Eli Lilly, Envivo/Forum, Genentech, Janssen/Johnson & Johnson, Lundbeck, Merck, Pfizer, Roche, TauRx, Vaccinex, and received consulting fees from Biogen, Cortexyme, Eisai, Medscape, Miller Communications, Prevail, and support for presentations from Biogen, Eisai, and Medscape. GYH acknowledges institutional support from Biogen, Cassava, Eli Lilly, Eisai, NIH, CIHR, and received consulting fees from Biogen, Eli Lilly, Eisai, NovoNordisk, Roche. MJ acknowledges institutional support from German Center for Neurodegenerative Diseases. JL acknowledges institutional support from German Ministry for Research and Education, Ehrmann Foundation, Lüneburg Foundation, InnovationsFonds, Michael J. Fox Foundation, CurePSP, Jerome Lejeune Foundation, Alzheimer Forschungs Initiative, Deutsche Stiftung Down Syndrom, Else Kröner Fresenius Stiftung, DZNE MODAG GmbH, DFG (XC 2145 SyNergy – ID 390857198), and received consulting fees from Eisai, and Biogen, support for presentations from Bayer Vital, Biogen, Eisai, TEVA, Roche, Esteve, Zambon, support for attending meetings from Abbvie, and involvement in patents EP 23 156 122.6 and EP 22 159 408.8. MM acknowledges institutional support from Canadian Institutes of Health Research, Weston Brain Institute, Ontario Brain Institute, Brain Canada, Roche, Alector, and received consulting fees from Arkuda Therapeutics, Ionis, Alector, Wave Life Sciences, Biogen Canada, support for presentations from Alcetor, Arkuda Therapeutics. JMR acknowledges institutional support from NIH (R01AG06901), Avid Pharmaceuticals, AltaMed, CurePSP. JS acknowledges institutional support from NIH, Roche, Lilly, Johnson & Johnson, Eisai, and received consulting fees from Eisai, Roche. SS acknowledges institutional support from Biogen, Eisai, Genentech, Roche, CognitionRx, Lilly, Janssen, and received

This article is protected by copyright. All rights reserved.

consulting fees from Abbvie, Acumen, Alector, Biogen, Biohaven, Cognition, Eisai, Fujirebio, Genentech, Kisbee, Labcorp, Lilly, Merck, Neurophet, NovoNordisk, Prothena, Quest, Roche, and support for meeting attendance from Abbvie, Acumen, Lilly, Neurophet. PRS acknowledges institutional support from NIH, Anonymous Foundation, Roth Charitable Foundation, NHMRC, MRFF, and received consulting fees from Outside Opinion Pty Ltd, Moira Clay Consulting Pty Ltd, Neuroscience Research Australia. CHvD acknowledges institutional support from Lilly, Roche, Biogen, Genentech, Eisai, UCB, Cerevel, Janssen, and received consulting fees from Eisai, Roche, Ono, Cerevel. GK acknowledges employment and stock incentives at F Hoffman La Roche at time of study. DBC received consulting fees from Seagen Inc, Roche, and payment for services from NYU Langone Med. Ctr., Loughren, Loughren, & Loughren PC, Powell Gilbert LLP. CC acknowledges institutional support from NIH, Alzheimer's Association, Michael J. Fox Foundation, and received consulting fees from Circular Genomics, Alector, and leadership and stock incentives at Vivid Genetics, Circular Genomics. JH received consulting fees from Prothena, AlzPath. EM acknowledges institutional support from NIH (U19AG032438, U01AG059798, R13AG055232, K-award), Alzheimer's Association, and received payment for services from Eisai, AAN, and financial incentives from C2N diagnostics. JCM acknowledges institutional support from NIH (P30 AG066444, P01AG003991, P01AG026276), and received consulting fees from Barcelona Brain Research Center, Native Alzheimer Disease-Related Resource Center in Minority Aging Research, and payment for presentations from AAIM, Int'l Brain Health Symposium. RJP acknowledges institutional support from NIH. CX acknowledges institutional support from NIH, and received consulting fees from Diadem. RJB acknowledges institutional support from NIH, GHR Foundation, Alzheimer's Association, DIAN-TU Pharma Consortium, and receives financial incentives from C2N Diagnostics, support for presentations

This article is protected by copyright. All rights reserved.

Author Manuscript

from the Korean Dementia Assn., American Neurological Assn., Weill Cornell Medical College, Fondazione Prada, Harvard University, University of Pennsylvania, involvement in US patents 12/267,974; 13/005,233; 62/492,718; 16/610,428; 17/015,985; 15/515,909, leadership role in C2N Diagnostics, and receipt of equipment and materials from Eisai, Janssen, Hoffman La Roche. TLSB acknowledges institutional support from Siemens, and received consulting fees from Biogen, Eli Lilly, Eisai, Bristol Myers Squibb, Johnson & Johnson, Merck, MedScape, PeerView, involvement in US patents 16/097,457; 12/016,701, and receipt of equipment and materials from Avid Radiopharmaceuticals/Eli Lilly, LMI, Lantheus, Hyperfine. The other authors report no conflicts of interest.

Figure Caption

Author Manuscript

This article is protected by copyright. All rights reserved.

Author Manuscript

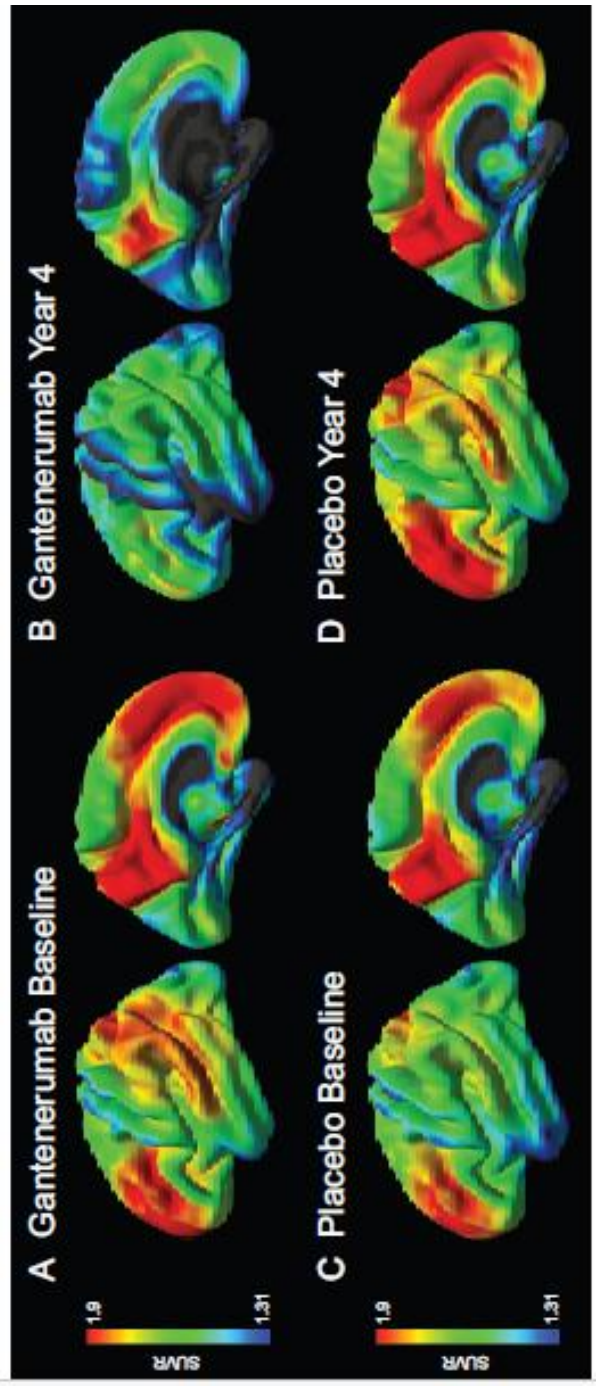


Fig. 1. Voxel-wise mean PiB PET SUVR levels in 4-year completer participants by drug status. Voxel-wise mean PiB PET SUVR levels across the subset of participants who completed the 4-year trial course at A) baseline (year 0) in the drug group, B) year 4 in the drug group, C) baseline (year 0) in the placebo group, and D) Year 4 in the placebo group. In order to visualize voxel-wise results non-partial-volume corrected data was used.

This article is protected by copyright. All rights reserved.

Author Manuscript

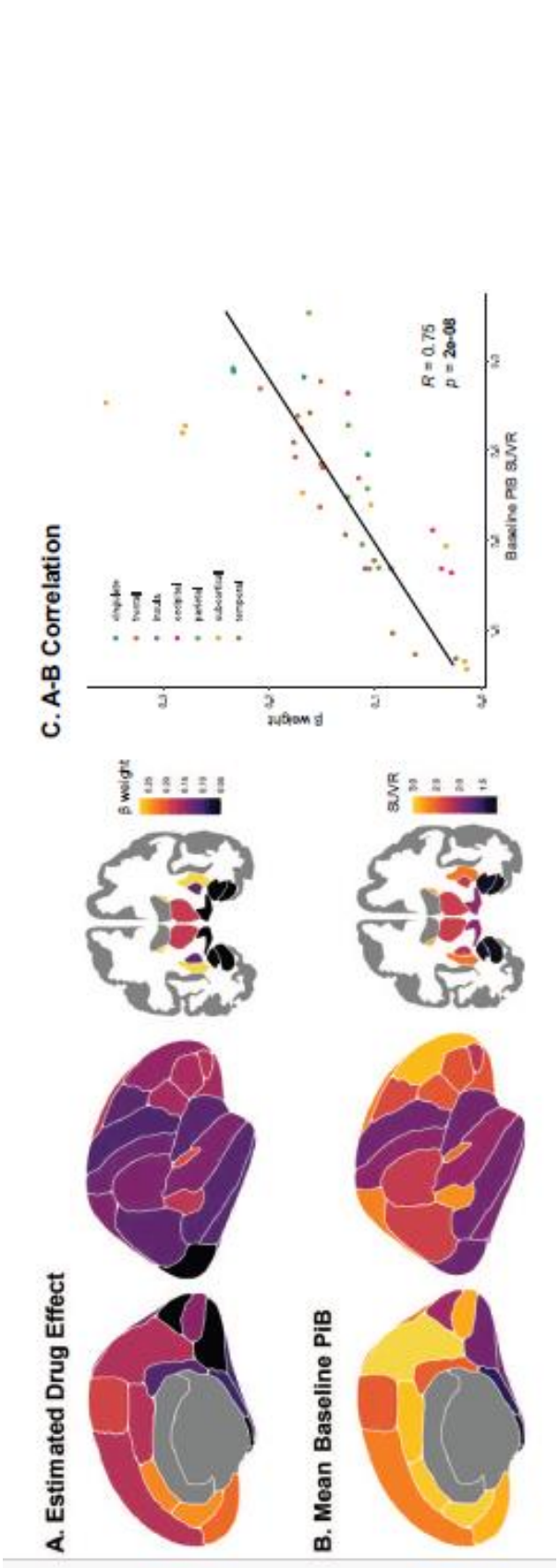


Fig. 2. Regional differences in estimated drug effect on PiB PET signal levels. A) Regional linear mixed effects models were used to estimate the effect of longitudinal Gantenerumab use on PiB PET signal. Regional PiB PET signal was dependent variable, with fixed effects covariates age, sex, CDR, ApoE4 status, and drug x time interaction term, and subject specific random slopes and intercepts were modeled. A) Beta weights for the drug x time interaction term are displayed. B) Regional mean baseline PiB PET signal for trial participants. C) Pearson

This article is protected by copyright. All rights reserved.

correlation between the regional estimated drug effect beta weights and baseline PiB PET pathology levels observed. Colors classify each region by spatial location in the brain.

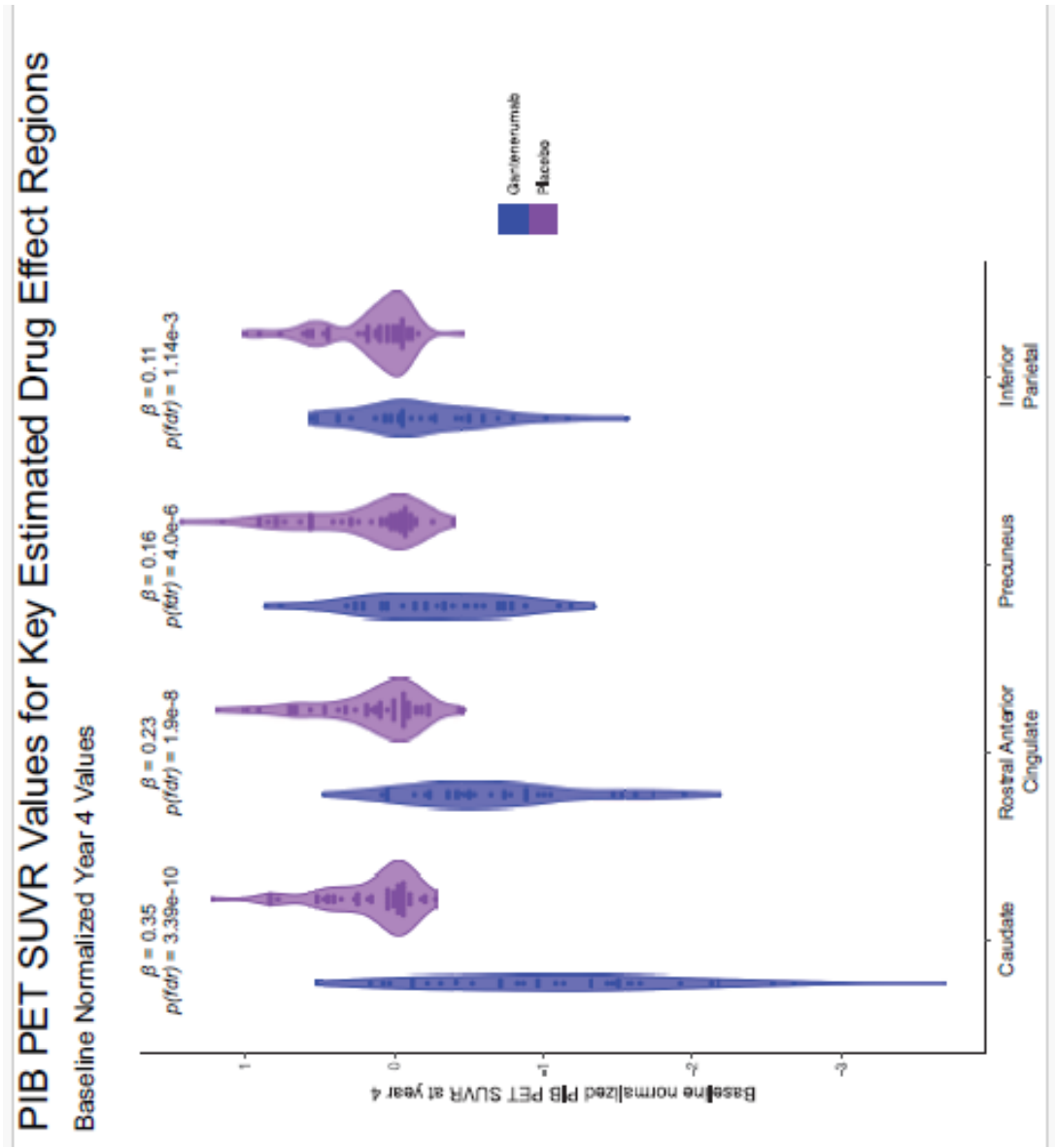


Fig. 3. PiB PET SUVR Values for Key Estimated Drug Regions. Baseline normalized PiB PET SUVR values at end-of-trial (year 4) for a subcortical high estimated drug effect region (caudate), a cortical high estimated drug effect region (rostral anterior cingulate), a key region in DIAD amyloid pathology (precuneus), and a cortical region with much lower estimated drug effect results (inferior parietal) are shown to demonstrate region specific amyloid clearance rates. Longitudinal mixed effects model β weights and p values for each region are listed for context.

This article is protected by copyright. All rights reserved.

Author Manuscript

Table 1 – Baseline participant characteristics

	Active gantenerumab	Placebo
N	52	40
Age (mean ± SD, years)	46.0 ± 10.8	44.2 ± 9.6
Female (n (%))	21 (40)	22(55)
APP mutation carrier (n (%))	6 (12)	5 (13)
PSEN1 mutation carrier (n (%))	43 (83)	32 (80)
PSEN2 mutation carrier (n (%))	3 (6)	3 (8)
APOE-ε4 carrier (n (%))	16 (31)	13 (32)
EYO (mean ± SD, years)	-3.5 ± 7.1	-3.5 ± 7.6
CDR 0 (n (%))	31 (60)	22 (55)
CDR 0.5 (n (%))	15 (29)	15 (38)
CDR 1 (n (%))	6 (12)	3 (8)
CDR-SB (mean ± SD)	1.33 ± 2.08	1.43 ± 1.87
Digit symbol (mean ± SD)	46.96 ± 20.56	46.63 ± 19.12
MMSE (mean ± SD)	27.10 ± 3.45	26.68 ± 3.97
Logical memory (mean ± SD)	9.90 ± 6.33	9.40 ± 6.45
ISLT (mean ± SD)	5.96 ± 4.04	5.80 ± 4.42
Aβ burden (mean ± SD, PiB-PET composite SUVR)	2.64 ± 1.23	2.62 ± 1.20
Aβ burden (mean ± SD, Centiloid units)	64.75 ± 51.87	63.97 ± 49.46

Annotations: SD = standard deviation, APOE-ε4 = Apolipoprotein-E allele ε4, EYO = Estimated years to symptom onset, CDR = clinical dementia rating, CDR-SB = clinical dementia rating sum of boxes, MMSE = mini-mental state examination, ISLT = International Shopping List Test,

This article is protected by copyright. All rights reserved.

Author Manuscript

PiB = Pittsburg Compound B, PET = positron emission tomography, SUVR = standardized uptake value ratio.

Table 2 – Longitudinal participant data totals for each neuroimaging modality

Modality	Baseline	Year 1	Year 2	Year 4
PIB PET				
Gantenerumab	51	48 (5.8)	44 (13.7)	35 (31.3)
Placebo	40	37 (7.5)	34 (15)	26 (35)
FDG PET				
Gantenerumab	49	48 (2)	43 (12.2)	38 (22.4)
Placebo	35	35 (0)	30 (14.3)	25 (28.6)
MRI				
Gantenerumab	52	52 (0)	48 (7.7)	40 (23.1)
Placebo	40	40 (0)	36 (10)	31 (22.5)

Data represents the total number of scans used for analysis in each modality at baseline, year 1, year 2, and year 4 respectively. Numbers in parentheses denote the percentage of dropout relative to baseline at each time point. Dropout in this trial occurred for two main reasons: 1) Advancing pathology of participants coupled with relatively high patient burden of PET imaging, and 2) quality control failures during rigorous review.

Table 3 – Regional LME model outputs for the drug arm × time in study model component

Region name	Component estimate (β)	Standard error	Degrees of freedom	*t* value	FDR *P*-value
Summary Metric Models					
mean cortical	-0.15	0.02	71.08	-5.87	**1.28E-07**
Subcortical Region Models					
caudate	-0.35	0.04	77.03	-7.91	**3.39E-10**
putamen	-0.28	0.04	77.02	-8.05	**3.39E-10**
thalamus	-0.17	0.02	82.17	-6.92	**1.31E-08**

This article is protected by copyright. All rights reserved.

Author Manuscript

nucleus accumbens	-0.28	0.05	71.78	-5.76	**6.15E-07**
pallidum	-0.10	0.02	79.21	-4.58	**2.85E-05**
ventral diencephalon	-0.03	0.01	85.46	-2.31	**2.65E-02**
hippocampus	-0.01	0.01	229.06	-2.06	**4.47E-02**
amygdala	-0.02	0.01	74.59	-1.57	1.26E-01
brainstem	-0.01	0.01	81.00	-1.20	2.39E-01
Cortical Regions Models					
rostral anterior cingulate	-0.23	0.03	69.47	-6.89	**1.90E-08**
caudal anterior cingulate	-0.23	0.03	69.20	-6.88	**1.90E-08**
medial orbitofrontal	-0.21	0.03	77.45	-6.34	**1.02E-07**
paracentral	-0.18	0.03	78.56	-6.09	**2.10E-07**
insula	-0.11	0.02	78.47	-6.07	**2.10E-07**
parahippocampal	-0.08	0.01	77.39	-6.12	**2.10E-07**
lateral orbitofrontal	-0.15	0.03	77.63	-5.90	**3.93E-07**
superior frontal	-0.17	0.03	73.57	-5.80	**5.78E-07**
superior temporal	-0.13	0.02	69.54	-5.80	**6.01E-07**
transverse temporal	-0.18	0.03	71.57	-5.34	**3.11E-06**
precuneus	-0.16	0.03	70.19	-5.27	**4.00E-06**
posterior cingulate	-0.17	0.03	63.47	-5.26	**4.60E-06**
banks of the superior temporal sulcus	-0.16	0.03	59.43	-5.25	**5.15E-06**
pars opercularis	-0.15	0.03	66.72	-5.15	**5.68E-06**
precentral	-0.10	0.02	78.19	-5.00	**7.51E-06**
supramarginal	-0.13	0.03	60.01	-4.94	**1.32E-05**
fusiform	-0.09	0.02	63.26	-4.92	**1.32E-05**
pars orbitalis	-0.15	0.03	63.95	-4.87	**1.49E-05**
isthmus cingulate	-0.11	0.02	65.77	-4.75	**2.08E-05**
pars triangularis	-0.15	0.03	59.63	-4.76	**2.24E-05**
temporal pole	-0.06	0.01	72.32	-4.58	**3.12E-05**
superior parietal	-0.13	0.03	59.62	-4.59	**3.73E-05**
postcentral	-0.11	0.02	65.39	-4.52	**4.07E-05**
inferior temporal	-0.10	0.02	55.45	-4.39	**7.56E-05**
pericalcarine	-0.13	0.03	67.16	-4.30	**8.04E-05**
middle temporal	-0.11	0.02	57.28	-4.30	**9.38E-05**
rostral middle frontal	-0.15	0.04	63.10	-4.21	**1.12E-04**
caudal middle frontal	-0.12	0.03	65.76	-4.16	**1.21E-04**
frontal pole	-0.17	0.04	56.98	-3.91	**3.13E-04**
inferior parietal	-0.11	0.03	49.65	-3.52	**1.14E-03**
lingual	-0.04	0.01	63.02	-2.79	**8.27E-03**
cuneus	-0.05	0.02	48.30	-2.80	**8.41E-03**

This article is protected by copyright. All rights reserved.

Author Manuscript

entorhinal cortex	-0.02	0.01	65.89	-1.82	7.79E-02
lateral occipital	-0.03	0.03	34.52	-0.96	3.42E-01

Component estimates (β weights) represent the total effect of the predictor variable on longitudinal regional PiB PET signal over the trial period. Significant p values after false discovery rate (FDR) correction are in bold.

Highlights for: McCullough A, et al. Regional effects of gantenerumab on imaging biomarkers in the DIAN-TU001 trial

Gantenerumab unevenly decreased Aβ burden as measured by PiB-PET across brain regions.

Strongest decrease in PiB-PET uptake in basal ganglia and medial frontal structures.

Variable drug effect on Aβ partly due to the amount of burden present pre-treatment.

No regional effect on FDG-PET metabolism or MRI volumetrics after four years.

Research in Context for: McCullough A, et al. Regional effects of gantenerumab on imaging biomarkers in the DIAN-TU001 trial

1. Systematic review: The literature was reviewed using PubMed and appropriately cited trial studies of anti-amyloid immunotherapies. Gantenerumab, a monoclonal antibody targeting fibrillar amyloid-β, engaged its target. The primary imaging endpoint of global amyloid-β removal, estimated with PiB-PET, was reached in dominantly inherited Alzheimer's disease (DIAD).

This article is protected by copyright. All rights reserved.

Author Manuscript

2. Interpretation: We observed regional variability in amyloid-β removal by gantenerumab in DIAD participants. PiB-PET signal was most strongly reduced in basal ganglia and medial frontal structures, suggesting a regional susceptibility to amyloid-β plaque removal. For each region, this susceptibility was associated with the amyloid-β burden present pre-treatment. Removal of amyloid-β did not influence measures of brain metabolism or cortical atrophy, suggesting the need for a longer monitoring timeframe or larger effect.

3. Future directions: This study demonstrates regional variability in drug-effect of an anti-amyloid agent in DIAD and provides insights into the design of future clinical trials.

Author Manuscript

This article is protected by copyright. All rights reserved.